Evaluation of a nonpeptidic ligand for imaging of cholecystokinin 2 receptor expressing cancers

Charity Wayua, **Philip S. Low***

Department of Chemistry, Purdue University, 720 Clinic Drive, West Lafayette, IN 47907

Tel: (765) 494-5273. Fax: (765) 494-5272. E-mail:plow@purdue.edu.

ABSTRACT

Tumor-specific targeting ligands have recently been exploited to deliver both imaging and therapeutic agents selectively to cancer tissues *in vivo*. Because the cholecystokinin 2 receptor (CCK2R) is overexpressed in a variety of human cancers (e.g. lung, medullary thyroid, pancreatic, colon, and GIST), but displays limited expression in normal tissues, natural ligands of CCK2R have been recently explored for use in imaging CCK2R positive cancers. Unfortunately, results from these studies reveal that peptidic CCK2R ligands are not only unstable *in vivo*, but those ligands that mediate good uptake by tumor tissue also promote high retention of the radioimaging agent in the kidneys, probably due to capture of the conjugates by peptide scavenger receptors. In an effort to reduce normal organ retention of CCK2R-targeted drugs, we have synthesized a nonpeptidic ligand of CCK2R and examined its specificity for CCK2 receptors both *in vitro* and *in vivo.*

Methods: Nonpeptidic agonists and antagonists of cholecystokinin 2 receptor (CCK2R) described in the literature were evaluated for their affinities and specificities for CCK2R. Z-360, a benzodiazepine-derived CCK2R antagonist with subnanomolar affinity, was selected for complexation to ^{99m}Tc via multiple spacers. Following synthesis and purification, four complexes with different physicochemical properties were evaluated for binding to CCK2R-transfected HEK 293 cells. The best conjugate, termed CRL-3-^{99m}Tc, was injected into tumor-bearing mice containing CCK2R positive tumor xenografts and examined by gamma scintigraphy and SPECT-CT. Uptake of the conjugate in various organs was also quantified by tissue resection and gamma counting.

Results: CRL-3-^{99m}Tc was shown to bind with low nanomolar affinity to CCK2R *in vitro* and was localized to tumor tissue in athymic *nu/nu* mice implanted with CCK2R+ tumors. At 4 h post injection, tumor uptake was measured at 12.0±2.0 %ID/g tissue.

Conclusion: Because uptake of CRL-3-^{99m}Tc by nonmalignant tissues is negligible and since retention in the kidneys is only transient, we suggest that CRL-3-^{99m}Tc might constitute a useful radioimaging agent for detection, sizing and monitoring of CCK2R+ tumors.

Keywords: Tumor-targeted therapy, radioimaging of tumors, cholecystokinin 2/gastrin receptor, cancer imaging, nonpeptide, antagonist

INTRODUCTION

Overexpression of specific receptors on pathologic cell surfaces has been exploited for functional imaging of disease activity in both humans ((1-4)) and animal models of human disease ((5-7)). One such receptor, the cholecystokinin 2 receptor, (gastrin receptor, CCK2R) is a G-protein coupled receptor that is normally expressed in the central nervous system and the cells of the gastric mucosa ((8)). In the central nervous system, cholecystokinin (CCK) regulates appetite, pain, anxiety and wakefulness ((9, 10)). In the gastrointestinal tract, the closely related gastrin peptides modulate growth and differentiation of the gastric mucosa, and secretion of acid, bile and digestive enzymes ((11)).

CCK2R is also overexpressed in a number of cancers, where it is reported to mediate stimulation of cancer cell growth, migration ((12, 13)), metastasis ((14)), and survival ((15)). Those cancers shown to upregulate CCK2R include malignancies of the thyroid ((16)), lung ((17)), pancreas, ovary, brain ((18)), stomach, gastrointestinal stroma ((19)) and colon ((20)). Recently, a novel splice variant of CCK2R has also been identified that is tumor-specific and often co-expressed with the normal CCK2R spliceoform in malignant cells ((20, 21)). This splice variant, designated CCK2i4svR, results from retention of intron 4, which yields a modified receptor containing a 64 amino acid insertion in the third cytoplasmic domain. Importantly, this modified CCK2R is constitutively active ((22)), leading to increased basal cell proliferation and enhanced tumorigenicity, even in the absence of ligand ((23)).

The limited expression of CCK2R in normal tissues, coupled with the overexpression of CCK2R and CCK2i4svR in various cancers, has rendered the receptor an attractive

candidate for targeted imaging and therapy of malignant disease. Indeed, radioactive conjugates of CCK and gastrin have already been explored for use in imaging CCK2R overexpressing tumors in mice ((24-26)). Unfortunately, results from these studies have revealed inadequacies that suggest a need for improved CCK2R targeting ligands. First, gastrin peptides that exhibit high tumor uptake are also compromised by high retention in the kidneys, whereas CCK peptides that display low kidney uptake also show little retention in the tumors ((27-29)). As a consequence, development of CCK2R-targeted peptides for radiotherapeutic applications has been hampered by concerns that the targeted radiation might simultaneously cause damage to the kidneys. Second, gastrin and CCK, like most other peptide hormones, are rapidly degraded by peptidases in the serum and on cell surfaces ((30)), raising concern that attached cytotoxic cargos might be released during circulation, resulting in their nonspecific distribution into CCK2R negative tissues. Third, CCK/gastrin-related peptides are prone to oxidation at a methionine residue, leading to loss of receptor binding affinity and their consequent dissemination into receptor negative tissues ((30)). Finally, CCK and gastrin related peptides can stimulate growth, proliferation, and survival of cancer cells, rendering the tumor-targeted imaging agent an unwanted promoter of tumor growth.

To avoid the unwanted consequences associated with use of a peptidic agonist for tumor imaging, we have designed a nonpeptidic CCK2R targeting ligand and used it to deliver a ^{99m}Tc-based radioimaging agent to CCK2R positive cancers in tumor-bearing mice. We report here that this CCK2R-targeting ligand promotes tumor-specific accumulation of an attached radioimaging agent with low accumulation in normal tissues,

suggesting a possible use for the targeted imaging agent in detection, localization, and staging of CCK2R-expressing tumors.

METHODS

Chemicals

All amino acids and resins were purchased from Chem Impex Intl. Sodium pertechnetate (^{99m}Tc) was obtained from Cardinal Health. HC Matrigel was purchased from BD Biosciences. Stannous chloride, sodium glucoheptonate, diisopropylethylamine (DIPEA), piperidine, dimethylformamide (DMF), isopropyl alcohol and all other reagents were purchased from Sigma-Aldrich.

Cell culture and animal husbandry

Two HEK 293 cell lines, one transfected with CCK2R and the other expressing CCK2i4svR, were a kind gift from Dr. Mark Hellmich (University of Texas Medical Branch, Galveston, Texas). Cells were cultured in Dulbecco's Modified Eagles Media (GIBCO) supplemented with 10% fetal bovine serum, G418 disulfate (Sigma-Aldrich 400μg/ml) and 1% penicillin/streptomycin at 37 °C in a humidified 95% air/5% CO_2 atmosphere. Athymic female *nu/nu* mice were purchased from Harlan Laboratories, housed in a sterile environment on a standard 12 h light/dark cycle, and maintained on normal rodent chow. All animal procedures were approved by the Purdue Animal Care and Use Committee in accordance with NIH guidelines.

Synthesis of radioimaging agents

Z-360, a CCK2 receptor antagonist, was synthesized according to previously reported methods (*(31, 32)*) and linked via the desired spacer to a ^{99m}technetium chelating agent

after solid phase synthesis of the chelate-spacer conjugate. For this purpose, the chelator comprised of the peptide sequence β-L-diaminopropionic acid (β-DAP), L-aspartic acid (L-Asp), L-cysteine (L-Cys) was first prepared by solid phase methodology (*(33)*), after which the desired spacer was added (See Scheme 1).

The Z-360 ligand was then linked to the terminal amine and the final conjugate was cleaved from the resin and purified, as described below. Briefly, acid-sensitive Wang resin loaded with 0.106 mmol of H-carbonyl-trityl-L-cysteine (H-L-Cys(Trt)-OH) was reacted first with Fmoc-Asp(Otbu)-OH (0.265 mmol), HATU (0.265 mmol) and diisopropylethylamine (1.06 mmol) followed by addition of β-L-diaminopropionic acid (0.265 mmol), HATU (0.265 mmol) and diisopropylethylamine (1.06 mmol) to yield the ^{99m}Tc chelating moiety. The chelator was then conjugated to Z-360 via a variety of spacers that were selected for both their abilities to render the final conjugate water soluble and to reduce nonspecific binding to receptor negative cells (see Results). The monomeric components of these spacers were derived from protected amino acids and a peptidosaccharide construct described by others *(34)*. All conjugation reactions were performed under argon atmosphere. Fmoc protecting groups were removed after each coupling step using standard conditions (20% piperidine in dimethylformamide). Release of the partially deprotected conjugate from the polymeric support was finally accomplished by treatment with a solution of 92.5% trifluoroacetic acid (TFA), 2.5% 1,2-ethanedithiol, 2.5% triisopropylsilane, and 2.5% deionized water. This reaction also resulted in simultaneous removal of all *t*-butyl (*t*-Bu), *t*-butoxycarbonyl (*t*-Boc) and trityl protecting groups.

The crude product was purified by preparative reverse-phase high performance liquid chromatography (RP-HPLC) using a gradient mobile phase of A = 20 mM ammonium acetate buffer and B= acetonitrile; solvent gradient 5% B to 80% B in 30 minutes (Waters xTerra C18, 10μm; 19 x 250 mm). Elution of the conjugate was monitored at λ = 280 nm and the identities of the eluted compounds were analyzed by LC-MS and MALDI. Formulation and radiolabeling of the conjugates with ^{99m}Tc was performed according to previously described methods ((33)).

Binding affinity and specificity of the CCK2R ligand-^{99m}Tc conjugates

HEK 293 CCK2R and HEK 293 CCK2i4svR were seeded onto 24 well plates and grown to 80-90% confluence over 48-72 h. Spent media in each well was replaced with 0.5ml fresh media containing 0.5% bovine serum albumin and increasing concentrations of the radioconjugate were added. After incubating for 1 h at 37 °C, cells were rinsed with incubation solution (2 × 1.0 ml) and resuspended in 0.5 ml 0.25 N NaOH before radioactivity counting using a γ-counter. The dissociation constant (K_d) was calculated by plotting cell bound radioactivity as a function of the concentration of radiotracer in the media, assuming a non-cooperative single site binding equilibrium.

Analysis of tumor-bearing mice

Six-week-old female *nu/nu* mice (Harlan Laboratories, IN) were inoculated subcutaneously on their shoulders with either HEK 293 CCK2R or HEK 293 CCK2i4svR cells (5.0 × 10^6 cells/mouse in 50% HC Matrigel-DMEM media) using a 25-gauge needle. Growth of the tumors was measured in two perpendicular directions every 2 days using a caliper, and the volumes of the tumors were calculated with the formula, $0.5 \times L \times W^2$ (L = measurement of longest axis, and W = measurement of axis perpendicular to L

in millimeters). Radiotracer biodistribution studies were performed 12-18 days after tumor cell implantation, when the tumors had reached ~400-500 mm^3 in volume. The mice were randomly assigned to different treatment groups and injected intravenously with the desired ^{99m}Tc-labeled conjugate (10 nmol, 5.55 MBq (150 µCi) in 100 µl of phosphate buffered saline). At the indicated time points (0.5, 2, 4, 8 or 24 h after injection), animals were sacrificed by CO_2 asphyxiation, and imaging was performed using a KODAK Image Station. The parameters used for radioimaging were: acquisition time = 2 min, *f*-stop = 4, focal plane = 7, FOV = 200, binning = 4. For white light imaging, the parameters were: acquisition time = 0.05 s, *f*-stop = 11, focal plane = 7, FOV = 200, with no binning. SPECT/CT imaging was performed with a µSPECT II/CT (MILabs Utrecht, The Netherlands).

Biodistribution of radioimaging agents

After radioimaging, each animal was dissected and selected organs/tissues were collected into pre-weighed tubes and counted by γ-counting. CPM values were decay corrected and converted to % injected dose per gram of wet tissue (% ID/g).

RESULTS
#
Because of the limited expression of CCK2R in normal tissues coupled with its overexpression in a variety of tumors, we elected to develop a CCK2R-targeted ^{99m}Tc chelate complex that would not be encumbered by the specificity and stability problems associated with previous CCK2R-targeted peptidic radioimaging agents. Following an extensive literature search, we found a small molecule antagonist, Z-360 ((*35, 36*)), that binds CCK2R with subnanomolar affinity and high selectivity over the CCK1R (K_d=

0.47 nMol/L; selectivity over CCK1R = 672). Preferential binding to CCK2R was important, since CCK1R is highly expressed in several normal tissues ((*37*)). Moreover, ^{99m}Tc was chosen as the radiolabel due to its widespread availability, low cost, and short half-life (6.02 h).

For construction of the optimal CCK2R-targeted radioimaging agent, Z-360 was attached to a previously described ^{99m}Tc chelating agent ((*33*)) by a variety of spacers designed to both improve water solubility and prevent chelate complex interference with ligand binding. The final conjugates selected for comparison are shown in Fig. 1. Cholecystokinin receptor ligand 1 (CRL-1) contains a simple tripeptide spacer. Because scavenger receptors in the kidneys and liver can bind diverse peptidic conjugates ((*38, 39*)), the peptidic spacer in CRL-1 was replaced with a less readily scavenged peptidosaccharide (PS) spacer in CRL-2 (*39*). Next, to assure sufficient separation between the CRL ligand and its tethered radiochelate, CRL-3 was designed with the same spacer as CRL-2, only an octanoyl moiety was inserted before the peptidosaccharide spacer. Finally, to assist with evaluation of the impact of spacer length, CRL-4 was prepared with no spacer. Because the affinity of a ligand for its receptor can often be compromised by attachment to its cargo, the binding affinity of each of the above conjugates for both CCK2R and CCK2i4svR was examined *in vitro*. For this purpose, HEK 293 cells that had been transfected with either CCK2R or CCK2i4svR were incubated with increasing concentrations of each radioactive conjugate, both in the presence and absence of 100-fold excess of unlabeled CRL. Then, after washing to remove unbound conjugate, cell-associated radioactivity was determined by gamma counting. As seen in Fig. 2 and Table 1, CRL-1, CRL-2, and CRL-3 all showed high

affinity for both cell lines, with binding constants in the nanomolar range. In contrast, CRL-4 which contained no spacer displayed low affinity for both CCK2R and CCK2i4svR expressing cells, confirming the impact of spacer length on ligand affinity.

To determine the fraction of conjugate uptake that was receptor-mediated, parallel experiments were performed in the presence of 100-fold molar excess of unlabeled CRL to competitively block receptor binding. As revealed in Fig. 2, CRL-2 and CRL-3 showed quantitative competition upon addition of excess ligand, whereas CRL-4 and CRL-1 showed ~ 50% and ~20% residual non-specific binding, respectively. We suspect that the strong hydrophobicity of Z-360 favors membrane association for all conjugates, and that only the enhanced steric bulk and hydrophilicity of the peptidosaccharide spacers is sufficient to prevent nonspecific membrane association. The slightly higher affinity exhibited by CRL-3 compared to CRL-2 may be due to the increased separation of the binding ligand from the bulky peptidosaccharide spacer, however, additional subsite interactions may have also contributed to this difference in affinity. Based on these data, CRL-3 was selected for further testing in mice bearing both CCK2R and CCK2i4svR expressing tumor xenografts.

In vivo targeting and specificity of CRL-3-^{99m}Tc was next evaluated by injecting CRL-3-^{99m}Tc intravenously into athymic *nu/nu* mice bearing HEK-293 CCK2R and HEK- 293 CCK2i4svR tumor xenografts. As seen in Fig. 3, CRL-3-^{99m}Tc was observed to accumulate in HEK 293 CCK2R and HEK 293 CCK2i4svR tumors with little or no accumulation in other tissues except the kidneys (14.25% ID/g tissue, 2 h post injection). Pre-injection of the mice with 100-fold excess of unlabeled CRL conjugate was found to block tumor uptake, indicating that accumulation of the radiotracer in the malignant mass

was receptor-mediated (Fig. 4). In contrast, uptake of CRL-3-^{99m}Tc in the kidneys was not competable with excess CRL-3 (Fig.4), suggesting that the presence of CRL-3-^{99m}Tc in the kidneys does not depend on CCK2R expression.

Since small molecules are often excreted via the liver or kidneys (*(40)*), we determined whether uptake of CRL-3-^{99m}Tc in the liver and kidneys might be transient. As seen in the SPECT-CT images of Fig. 5, the CRL-3-^{99m}Tc content of the liver and kidneys decreased over time, whereas uptake in the tumor mass was relatively stable.

By 24 h post tail vein injection (Table 2), tumor to normal tissue ratios of CRL-3-^{99m}Tc in the muscle, heart, skin, blood, liver, and spleen were 90, 83, 30, 61, 4 and 14, respectively. These data suggest that ~~only~~ CCK2R+ tissues retain the accumulated CRL-3-^{99m}Tc in substantially greater quantities, and therefore, that any radiation damage to normal tissues should be minimal.

DISCUSSION

Overexpression of CCK2R in many malignant cells combined with its limited expression in normal tissues has suggested that CCK2R-targeted radioemitters might constitute attractive candidates for radioimaging of many human cancers. However, the very high uptake of natural ligands of CCK2R by the kidneys (in some cases ~60% of injected dose) (*29*) has strongly discouraged further investigation of peptides for this application. The objective of this paper was therefore to explore development of nonpeptidic ligands for imaging of cholecystokinin 2 receptor-expressing tumors. We show here that a small organic antagonist of CCK2R can be exploited to yield high

resolution images of CCK2R-expressing tumors, especially when time is allowed for the CRL conjugates to clear from the liver and kidneys. In addition to their avoidance of hepatic and renal retention, nonpeptidic CCK2R ligands may enable improved serum stability (*35*).

In order to evaluate the effect of spacer chemistry on CCK2R targeting, four different conjugates with distinct spacers were synthesized and evaluated. While each conjugate recognized both CCK2R and CCK2i4svR, CRL-3 displayed the highest affinity for both forms of the receptor, while CRL-4 showed the weakest affinity for the two receptors. Moreover, CRL-4 and to a lesser extent CRL-1 were both compromised by high nonspecific binding, suggesting a need for a hydrophilic spacer to offset the hydrophobicity of the core ligand, Z-360.   As seen in Fig. 2, binding of both peptidosaccharide-containing spacers could be nearly quantitatively blocked upon addition of excess ligand, suggesting almost exclusive receptor-mediated binding by these conjugates. CRL-3-^{99m}Tc also showed favorable pharmacokinetics *in vivo*, with rapid blood and kidney clearance, and sustained tumor retention.

Assuming that a CRL-targeted radio-/chemotherapeutic agent will display a similar biodistribution profile, possible use of CRL to target therapeutic payloads should not be ignored. Thus, the observed tissue distribution of CRL-3-^{99m}Tc implies that toxicity might be localized to the tumor, with negligible damage to normal tissues. Moreover, since kidney and liver accumulation are only transient, selection of a radiotherapeutic agent with a longer half-life might allow clearance of the radioactivity from the kidneys before significant decay of the radiotherapeutic conjugate has occurred in the tumor. In both radio- and chemotherapeutic applications, prior imaging of a patient

with CRL-3-^{99m}Tc might also prove useful in pre-selecting patients whose tumors express sufficient CCK2R to benefit from a CRL-targeted therapy.

CONCLUSION

In addition to targeting of radioimaging and chemotherapeutic agents, CRL might also be exploited to deliver other imaging modalities (e.g. PET, CT, optical and MRI contrast agents) selectively to CCK2R+ tumors. Furthermore, as shown for other tumor targeting ligands (*4, 7*), CRL might also be developed for delivery of fluorescent probes for use in fluorescence-guided resection of malignant masses during surgery (_ENREF_32). Fluorescent CRL conjugates might similarly be adapted for use in detection and capture of circulating tumor cells from the blood of cancer patients. In brief, if the tumor selectivity of CRL-3-^{99m}Tc is maintained with other conjugates of CRL, a variety of future clinical applications can be envisioned.

REFERENCES

1.   Ivancevic V, Wormann B, Nauck C, et al. Somatostatin receptor scintigraphy in the staging of lymphomas. *Leuk Lymphoma.* 1997;26:107-114.

2.   Nejmeddine F, Raphael M, Martin A, Le Roux G, Moretti JL, Caillat-Vigneron N. 67Ga scintigraphy in B-cell non-Hodgkin's lymphoma: correlation of 67Ga uptake with histology and transferrin receptor expression. *J Nucl Med.* 1999;40:40-45.

3.   Behr TM, Behe MP. Cholecystokinin-B/Gastrin receptor-targeting peptides for staging and therapy of medullary thyroid cancer and other cholecystokinin-B receptor-expressing malignancies. *Semin Nucl Med.* 2002;32:97-109.

4.   van Dam GM, Themelis G, Crane LMA, et al. Intraoperative tumor-specific fluorescence imaging in ovarian cancer by folate receptor-α targeting: first in-human results. *Nat Med.* 2011;17:1315-1319.

5.   Zhang J, Razavian M, Tavakoli S, et al. Molecular imaging of vascular endothelial growth factor receptors in graft arteriosclerosis. *Arterioscler Thromb Vasc Biol.* 2012;32:1849-1855.

6.   Vaitilingam B, Chelvam V, Kularatne SA, et al. A folate receptor-alpha-specific ligand that targets cancer tissue and not sites of inflammation. *J Nucl Med.* 2012;53:1127-1134.

7.   Kularatne SA, Zhou Z, Yang J, et al. Design, synthesis, and preclinical evaluation of prostate-specific membrane antigen targeted (99m)Tc-radioimaging agents. *Mol Pharm.* 2009;6:790-800.

8.   Mantyh CRP, Pappas TN, Vigna, SR. Localization of cholecystokinin A and cholecystokinin B/gastrin receptors in the canine upper gastrointestinal tract. *Gastroenterology.* 1994;107:1019-1030.

9.   Little TJ Horowitz M, Feinle-Bisset C. Role of cholecystokinin in appetite control and body weight regulation. *Obes Rev.* 2005;6:297-306.

10.   Bowers ME, Choi DC, Ressler KJ. Neuropeptide regulation of fear and anxiety: Implications of cholecystokinin, endogenous opioids, and neuropeptide Y. *Physiol Behav.* 2012;107:699-710.

11.   Dufresne M, Seva C, Fourmy D. Cholecystokinin and Gastrin Receptors. *Physiol Rev.* 2006;86:805-847.

12.   Noble PJ, Wilde G, White MR. Stimulation of gastrin-CCKB receptor promotes migration of gastric AGS cells via multiple paracrine pathways. *Am J Physiol Gastrointest Liver Physiol.* 2003;284:G75–84.

13.   Oikonomou E, Buchfelder M, Adams EF. Cholecystokinin (CCK) and CCK receptor expression by human gliomas: evidence for an autocrine/paracrine stimulatory loop. *Neuropeptides.* 2008;42:255–265.

14. Wroblewski LE Prtichard DM, Carter S, et al. Gastrin-stimulated gastric epithelial cell invasion: the role and mechanism of increased matrix metalloproteinase 9 expression. *Biochem J.* 2002;365:873-879.

15. Watson SA, Grabowska AM, El-Zaatari M, et al. Gastrin - active participant or bystander in gastric carcinogenesis? *Nat Rev Cancer.* 2006;6:936-946.

16. Reubi JC, Waser B. Unexpected high incidence of cholecystokinin B/gastrin receptors in human medullary thyroid carcinomas. *Int J Cancer.* 1996;67:644-647.

17. Sethi T, Herget M, Wu SV, et al. CCK-A and CCK-B receptors are expressed in small cell lung cancer lines and mediate Ca2+ mobilization and clonal growth. *Cancer Res.* 1993;53:5208-5213.

18. Reubi JC SJ, Waser B. Cholecystokinin(CCK)-A and CCK-B/gastrin receptors in human tumors. *Cancer Res.* 1997;57:1377-1386.

19. Hur K KM, Lee HJ, Park DJ, et al. Expression of gastrin and its receptor in human gastric cancer tissues. *J Cancer Res Clin Oncol.* 2006;132:85-91.

20. Körner M WB, Reubi JC, Miller LJ. CCK(2) receptor splice variant with intron 4 retention in human gastrointestinal and lung tumours. *J Cell Mol Med.* 2010;14:933-943.

21. Smith JP, Verderame, MF, McLaughlin P, et al. Characterization of the CCK-C (cancer) receptor in human pancreatic cancer. *Int J Mol Med.* 2002;10:689-694.

22. Olszewska-Pazdrak B Townsend Jr CM, Hellmich MR. Agonist-independent activation of Src tyrosine kinase by a cholecystokinin-2 (CCK2) receptor splice variant. *J Biol Chem.* 2004;279:40400-40404.

23. Chao C, Goluszko E, Lee Y-T, et al. Constitutively active CCK2 receptor splice variant increases Src-dependent HIF-1a expression and tumor growth. *Oncogene.* 2007;26:1013-1019.

24. Laverman P, Joosten L, Eek A, et al. Comparative biodistribution of 12 ^{111}In-labelled gastrin/CCK2 receptor-targeting peptides. *Eur J Nucl Med Mol Imaging.* 2011;38:1410-1416.

25. Laverman P, Roosenburg S, Gotthardt M, et al. Targeting of a CCK(2) receptor splice variant with (111)In-labelled cholecystokinin-8 (CCK8) and (111)In-labelled minigastrin. *Eur J Nucl Med Mol Imaging.* 2008;35: 386-392.

26. Aloj L, Aurilio M, Rinaldi V, et al. Comparison of the binding and internalization properties of 12 DOTA-coupled and ^{111}In-labelled CCK2/gastrin receptor binding peptides: a collaborative project under COST Action BM0607. *Eur J Nucl Med Mol Imaging.* 2011;38:1417-1425.

27. Behr TM, Jenner N, Radetzky S, et al. Targeting of cholecystokinin-B/gastrin receptors in vivo: preclinical and initial clinical evaluation of the diagnostic and therapeutic potential of radiolabelled gastrin. *Eur J Nucl Med.* 1998;25:424-430.

28.   Behr TM, Béhé M, Angerstein C, et al. Cholecystokinin-B/gastrin receptor binding peptides: preclinical development and evaluation of their diagnostic and therapeutic potential. *Clin Cancer Res.* 1999;5:3124s-3138s.

29.   Béhé M, Kluge G, Becker W, et al. Use of polyglutamic acids to reduce uptake of radiometal-labeled minigastrin in the kidneys. *J Nucl Med.* 2005;46:1012-1015.

30.   Ocak M, Helbok A, Rangger C, et al. Comparison of biological stability and metabolism of CCK2 receptor targeting peptides, a collaborative project under COST BM0607. *Eur J Nucl Med Mol Imaging.* 2011;38:1426-1435.

31.   Lauffer D.J. Mullican MD. A practical synthesis of (S) 3-tert-Butoxycarbonylamino-2-oxo-2,3,4,5-tetrahydro-1,5-benzodiazepine-1-acetic acid methyl ester as a conformationally restricted dipeptido-Mimetic for caspase-1 (ICE) inhibitors. *Bioorg Med Chem Lett.* 2002;12:1225-1227.

32.   Wayua C, Low PS. Evaluation of a cholecystokinin 2 receptor-targeted near-infrared dye for fluorescence-guided surgery of cancer. *Mol Pharm.* 2014;11:468-476.

33.   Leamon CP Parker MA, Vlahov IR, et al. Synthesis and biological evaluation of EC20: a new folate-derived, (99m)Tc-based radiopharmaceutical. *Bioconjug Chem.* 2002;13:1200-1210.

34.   Vlahov IR, You F, Wang Y, et al. Carbohydrate-based synthetic approach to control toxicity profiles of folate-drug conjugates. *J Org Chem.* 2010;75:3685-3691.

35.   Kawasaki D, Emori Y, Eta R, et al. Effect of Z-360, a novel orally active CCK-2/gastrin receptor antagonist on tumor growth in human pancreatic adenocarcinoma cell lines in vivo and mode of action determinations in vitro. *Cancer Chemother Pharmacol.* 2008;61:883-892.
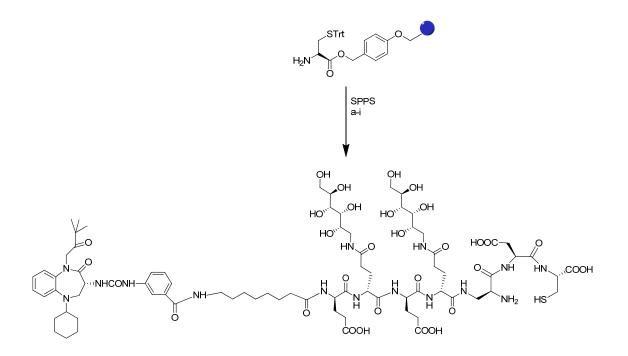
36.   Grabowska AM, Morris TM, McKenzie AJ, et al. Pre-clinical evaluation of a new orally-active CCK-2R antagonist, Z-360, in gastrointestinal cancer models. *Regulatory Peptides.* 2008;146:46-57.

37.   Monstein HJ Nylander AG, Salehi A, et al. Cholecystokinin-A and cholecystokinin-B/gastrin receptor mRNA expression in the gastrointestinal tract and pancreas of the rat and man. A polymerase chain reaction study. *Scand J Gastroenterol.* 1996;31:383-390.

38.   Vegt E, Melis M, Eek A, et al. Renal uptake of different radiolabelled peptides is mediated by megalin: SPECT and biodistribution studies in megalin-deficient mice. *Eur J Nucl Med Mol Imaging.* 2011;38:623-632.

39.   Leelahavanichkul A, Bocharov AV, Kurlander R, et al. Class B scavenger receptor types I and II and CD36 targeting improves sepsis survival and acute outcomes in mice. *J Immunol.* 2012;188:2749-2758.

40.   Maack J, Johnson V, Kan T, et al. Renal filtration, transport, and metabolism of low molecular weight proteins: A review. *Kidney Int.* 1979;16:251-270.

Scheme 1. Solid phase synthesis of CRL-3. All reactions were conducted under N_2 or Ar at room temperature. Reagents and conditions of reactions a-i are: (a) Fmoc-Asp(OtBu)-OH, HATU, DIPEA, 4h; b) (i) 20% piperidine/DMF, 10 min; (ii) Fmoc-diaminopropionic (DAP) acid, HATU, DIPEA, 4 h; c) (i) 20% piperidine/DMF, 10 min; (ii) 3,4,5,6-di-isopropylidene-1-amino-deoxy(Fmoc-Glu-OH)-D-glucitol, HATU, DIPEA, 4 h; d) (i) 20% piperidine/DMF, 10 min; (ii) Fmoc-Glu(OtBu)-OH, HATU, DIPEA, 4 h; e) (i) 20% piperidine/DMF, 10 min; (ii) 3,4,5,6-di-isopropylidene-1-amino-deoxy(Fmoc-Glu-OH)-D-glucitol, HATU, DIPEA, 4 h; f) (i) 20% piperidine/DMF, 10 min; (ii) Fmoc-Glu(OtBu)-OH, HATU, DIPEA, 4 h; g) (i) 20% piperidine/DMF, 10 min; (ii) Fmoc-8-amino-octanoic , HATU, DIPEA, 4 h; h) (i) 20% piperidine/DMF, 10 min; Z-360, HATU, DIPEA, overnight; i) cleavage in TFA/H_2O/TIPS/EDT (92.5:2.5:2.5:2.5), 30 min.
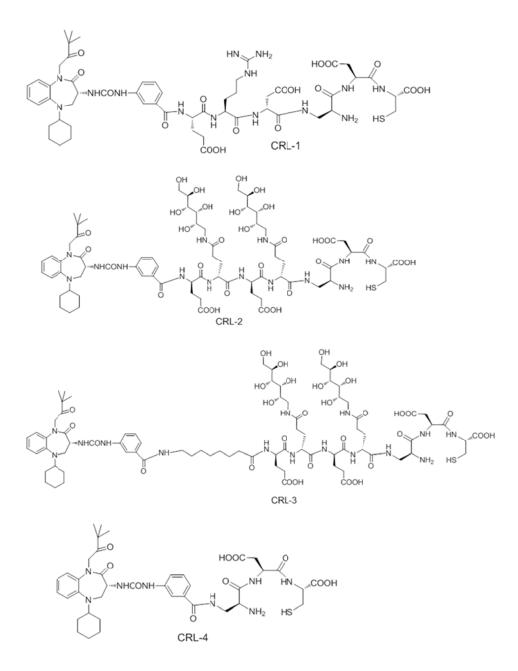
18

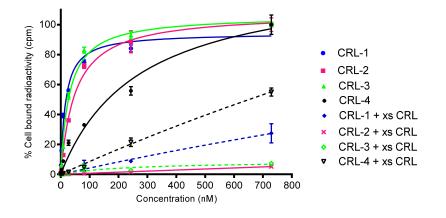**FIGURE 1.** Structures of CRL-targeted radioimaging conjugates

FIGURE 2. *In vitro* binding isotherms of CRL-1, CRL-2 and CRL-3 for HEK 293 CCK2R cells in the absence (——) and presence (-----) of 100-fold molar excess of unlabeled CRL. Error bars indicate s.d. (n=3)
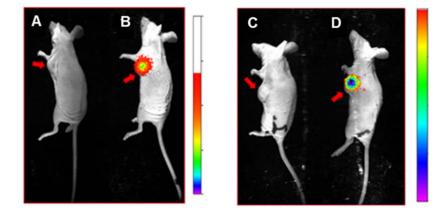
FIGURE 3. Evaluation of the specificity of CRL-3-^{99m}Tc for CCK2R-expressing tumors in tumor-bearing mice. Overlay of whole body radioimages (rainbow colors) on white light photographs of *nu/nu* mice bearing HEK CCK2R (a, b) and HEK CCK2i4svR (c,d) tumor xenografts in the presence (a, c) and absence (b, d) of 100-fold molar excess of CRL-3. Two hours after tail vein administration of 5.55 MBq CRL-3-^{99m}Tc, mice were euthanized and kidneys were shielded with a lead plate in order to allow easier visualization of the radioconjugate in other tissues. Red arrows indicate location of the tumor.
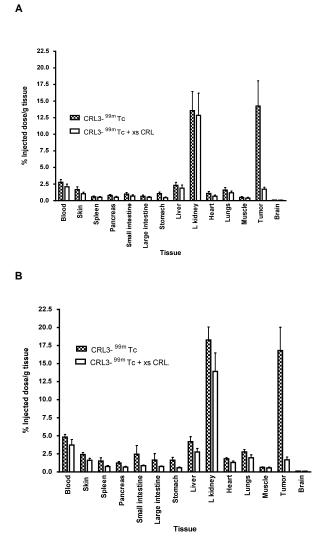
A

B

FIGURE 4. Tissue distribution of CRL-3-^{99m}Tc in *nu/nu* mice bearing (a) HEK CCK2R, and (b) HEK CCK2i4svR tumor xenografts 2 h post injection of 5.55 MBq CRL-3-^{99m}Tc. Error bars represent s.d. (n= 5 mice/group).
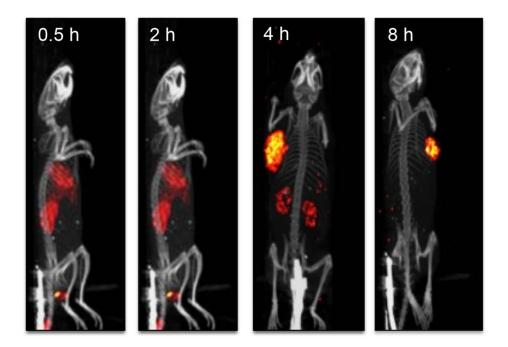
FIGURE 5. Examination of the rate of clearance of CRL-3- ^{99m}Tc from tumor-bearing mice using SPECT/CT. Mice implanted with HEK CCK2R tumor xenograft were injected with 5.55 MBq CRL-3- ^{99m}Tc and imaged 0.5, 2, 4, and 8 h post tail vein injection.

TABLE 1. Binding affinities of CRL-targeted radioimaging agents in HEK 293 CCK2R and HEK 293 CCK2i4svR cells.

Compound	Kd (nM) HEK 293 CCK2R Cells	Kd (nM) HEK 293 CCK2i4svR cells
CRL-1	**16**	*
CRL-2	**46 31**	
CRL-3	**30 4**	
CRL-4	**270**	*

*K_d could not be determined due to the very high nonspecific binding of CRL-1 and CRL-4 and the significantly lower number of receptors present on cells expressing CCK2i4svR.

Organ	0.5 h	2 h	4 h	8 h	24 h
Blood	5.8 ±2.7	1.9±0.97	1.7±0.39	0.24±0.19	0.10±0.06
Skin	2.3±1.2	1.0±0.41	1.1±0.23	0.42±0.22	0.21±0.13
Spleen	2.1±1.2	0.69±0.70	1.4±0.41	0.65±0.42	0.45±0.39
Pancreas	1.3±0.62	0.69±0.84	0.29±0.19	0.10±0.06	0.053±0.03
Small Intestine	1.2±0.63	0.52±0.28	0.52±0.08	0.19±0.10	0.13±0.08
Large Intestine	1.0±0.52	0.46±0.20	0.53±0.11	0.24±0.16	0.13±0.08
Stomach	1.2±0.61	0.58±0.32	0.56±0.16	0.24±0.15	0.15±0.09
Liver	6.7±3.6	2.5±2.4	4.1±0.64	1.9±1.2	1.4±1.4
Left Kidney	11.2±6.1	8.4±4.6	13.4±2.1	6.0±3.1	2.6±1.6
Right Kidney	11.4±6.3	7.6±4.4	12.8±1.8	5.7±3.0	2.6±1.7
Heart	2.3±1.5	0.68±0.47	0.59±0.18	0.14±0.078	0.076±0.05
Lungs	3.2±1.7	1.2±0.55	1.0±0.23	0.29±0.15	0.18±0.12
Muscle	0.8±0.4	0.29±0.096	0.3±0.04	0.093±0.048	0.070±0.08
Brain	0.13±0.07	0.051±0.02	0.053±0.016	0.064±0.12	0.0076±0.005
Tumor	7.4±4.6	8.1±5.1	12.0±2.0	8.5±4.9	6.3±3.7

TABLE 2. Tissue distribution of CRL-3- ^{99m}Tc in mice with subcutaneous HEK 293 – CCK2R cells at 0.5, 2, 4, 8 and 24 h post injection. Uptake of radioactivity is expressed as percent injected dose per gram of wet tissue. (n=5 for hours 0.5, 4, 8, and 24; n=10 for hour 2 time point).